SpezialForschungsBereich F 32

Karl–Franzens Universität Graz
Technische Universität Graz
Medizinische Universität Graz

Magnetic Induction Tomography: The influence of the coil configuration on the spatial resolution

R. Merwa H. Scharfetter

SFB-Report No. 2007–011 December 2007

A–8010 GRAZ, HEINRICHSTRASSE 36, AUSTRIA

Supported by the
Austrian Science Fund (FWF)

SFB sponsors:

- **Austrian Science Fund** (FWF)
- **University of Graz**
- **Graz University of Technology**
- **Medical University of Graz**
- **Government of Styria**
- **City of Graz**

Magnetic InductionTomography: The influence of the coil configuration on the spatial resolution

R. Merwa[1] and H. Scharfetter[1]

[1] Institute of Medical Engineering, Graz University of Technology, Kronesgasse 5, 8010 Graz, Austria

Abstract—**Magnetic Induction Tomography (MIT) is a low-resolution and contact-less imaging modality for mapping the electrical properties inside a region of interest. For an imaging system it is necessary to give forecasts about the quality of an image. This paper is dedicated to investigate the resolution and location of a inhomogeneity subject to the number and to the location of the used excitation coils and receiving coils around the region of interest. To this end the Point-Spread-Function (PSF) was calculated for different coil configurations and with 40 dB signal-to-noise ratio. In analogy to EIT the PSF depends on the location and shows the broadest distribution in the centre of the object. The results show that the resolution depends on the used coil configuration especially the location of the coils with respect to each other and increases, when moving from the centre towards the border of the object.**

Keywords—**magnetic induction tomography, point spread function, resolution, coil configuration, regularization**

I. INTRODUCTION

MIT [1], [3], [5], [8] images the electrical characteristics, especially the conductivity distribution within an object under investigation. This technique is similar to the method of Electrical Impedance Tomography but avoids the ill-defined electrode skin interface due to the contactless operation by means of excitation and receiving coils. The primary magnetic field produced by a system of excitation coils causes an eddy current field inside the conducting region. The primary and secondary field are detected with an array of receiving coils around the object and the induced voltages carry the information about the conductivity distribution inside the object. The evaluation of the image quality has been described basically in [6] but only for a MIT system with 16 excitation and 32 receiving coils. This paper is dedicated to analyse the resolution and the location (especially the displacement) of an inhomogeneity in 3D for different coil arrangements by means of varying the numbers and positions of the used coils.

II. METHODS

A. Modelling setup

The 3D software phantom depicted in figure 1 comprises an array of 16 excitation coils and 32 receiving coils and a conducting cylinder with a radius of 95 mm and a height of 110 mm. The conductivity of the cylinder was 0.1 S/m, the permittivity was 80 and the excitation frequency was 100 kHz. The rectangular receiver coils had edge lengths of 38.7 mm and 20 mm and were placed on two parallel rings with a radius of 110 mm whereas each ring comprises 16 evenly spaced coils. The excitation coils had a diameter of 110 mm, a height of 20 mm and a thickness of 1 mm and they were arranged on a ring with a radius of 145 mm around the conducting cylinder.

B. Point-Spread-Function (PSF)

The PSF defines the propagation in an image due to a point source and we characterized the resolution of MIT with the Raleigh criterion. In case of a sinc-shaped PSF the lowest separable distance is equivalent to the 64%-width of the PSF. In this paper the object is the model cylinder and the PSF is calculated by mapping the true parameter values $\Delta\kappa_t$ to the reconstructed values $\Delta\kappa_r$ using the equation

$$\Delta\kappa_{\mathbf{r}} = \mathbf{A}\mathbf{S}\Delta\kappa_t = \mathbf{M}\Delta\kappa_t \tag{1}$$

The pseudo inverse $\mathbf{A}$ for the regularized problem using the unit matrix as the regularization matrix is defined as

$$\mathbf{A} = \left(\mathbf{S}^T\mathbf{S} + \lambda\mathbf{E}\right)^{-1}\mathbf{S}^T \tag{2}$$

$\mathbf{S}$ is the sensitivity matrix and λ is the regularization parameter. The PSF for the i_{th} voxel is the 3D map of the i_{th} column of the matrix $\mathbf{M}$ in (1) [4].

C. Regularization

A major question for a defined noise level is: What is the detactable size of an inhomogeneity with a given contrast at a certain position? Different noise levels require different values of the regularization parameter in order to

Hermann Scharfetter, Robert Merva (Eds.): ICEBI 2007, IFMBE Proceedings 17, pp. 456–459, 2007
www.springerlink.com © Springer-Verlag Berlin Heidelberg 2007

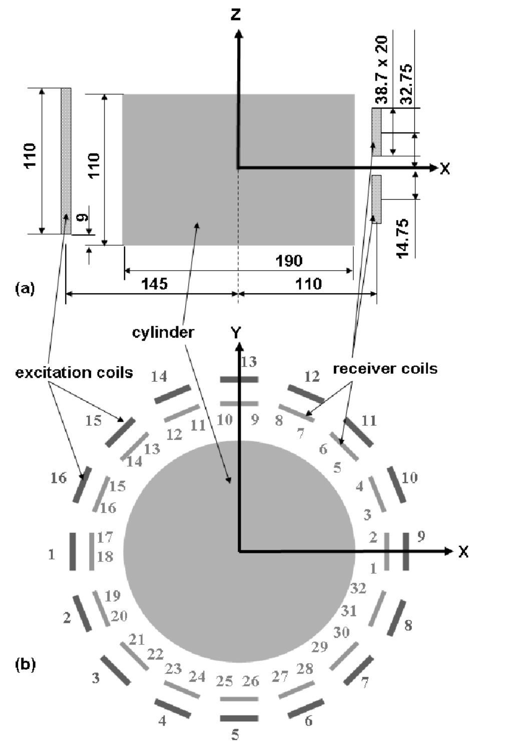

Fig. 1 Simulation arrangement for solving the inverse problem and generating simulated measuring data, (a) front view, (b) top view, all measures in mm

obtain satisfying images. There are several methods for the determination of the regularization parameter and in our case we use the Morozov discrepancy principle described in [2]. The basic idea of this method is, that the random error in the approximated solution cannot be less than in the data. The regularization parameter λ was calculated for a signal-to-noise ratio (SNR) of 40 dB.

D. Signal-to-noise ratio (SNR)

The SNR is defined as

$$SNR = 20log_{10}\frac{U_S}{U_N} \tag{3}$$

with U_S is the signal voltage and U_N is the noise voltage. 1 % (SNR=40 dB) of the maximum of all ΔV_i due to the perturbation was added to the simulated voltage data as uncorrelated Gaussian noise.

E. Simulation and Evaluation

The resolution and the correctness of the location were calculated on a finite element grid (about 20000 tetrahedral finite elements of second order) for different coil arrangements and were then mapped to a cubic grid with a spacing of 5 mm. Mapping was achieved by simply assigning the value in the respective finite element to the nearest cube. "Nearest" in this context means that the distance between the centres of gravity is minimal.

The resolution for the particular voxels was calculated by means of the 64%-width of the PSF ($resolution = 1/width_{PSF}$ $[mm^{-1}]$) as a function of the radius of the cylinder.

The following simulations were performed:

- Calculation of the PSF for all cubic voxels at the position x=[-90:5:90], y=[-90:5:90] and z=[-50:5:50] [mm] for each regularization method with a SNR of 40 dB and for the coil arrangements with the following abbreviations: E# is the number of the excitation coils, R#R1 and R#R2 are the numbers of the receiving coils arranged on two different rings R1 and R2 with respect to the excitation coils. Receiving coils on the ring R1 are partially directly in front of the excitation coils and the ring R2 is rotated with 22.5 degree with respect to R1. N1 means that 1% noise corresponding to 40 dB signal-to-noise rato was added to the measurement data and EM is the abbreviation for the regularization with the unit matrix.
- Coil arrangement E16
  Exc coil: 1 to 16
- Coil arrangement E8
  Exc coil: 1,3,5,7,9,11,13,15
- Coil arrangement E4
  Exc coil: 1,5,9,13
- Coil arrangement R32
  Rec coil: 1 to 32
- Coil arrangement R16R1
  Rec coil: 1,2,5,6,9,10,13,14,17,18,21,22,25,26,29,30
- Coil arrangement R16R2
  Rec coil: 3,4,7,8,11,12,15,16,19,20,23,24,27,28,31,32
- Coil arrangement R8R1
  Rec coil: 1,2,9,10,17,18,25,26
- Coil arrangement R8R2
  Rec coil: 3,4,11,12,19,20,27,28

The following evaluations were performed:

- Evaluation of the resolution of the PSF.
- Evaluation of the correctness of the location of the voxel.

Correctness in this context means the displacement of the obtained 64%-PSF-width from the original voxel position. The shift of the voxels in the PSF image was determined by localizing the centre of gravity in the neighborhood of

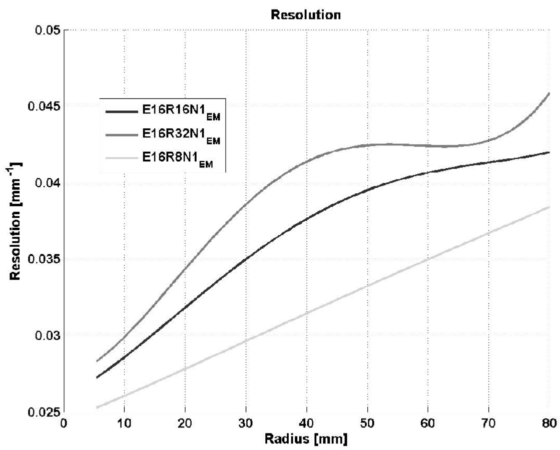

Fig. 2 Resolution in mm^{-1} as a function of the radius of the cylinder with 16 excitation coils, different configurations for the receiving coils and a SNR of 40 dB in the z-plane at z=0

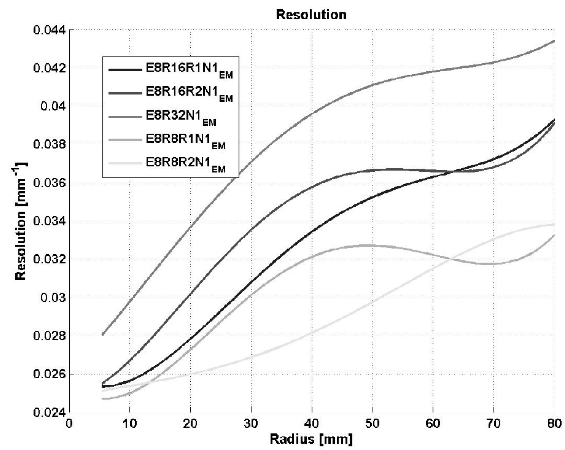

Fig. 3 Resolution in mm^{-1} as a function of the radius of the cylinder with 8 excitation coils, different configurations for the receiving coils and a SNR of 40 dB in the z-plane at z=0

the original position of the voxel. For the calculation an iterative algorithm is used which calculates the centre of gravity of all finite elements which are inside a sphere with a radius of 15 mm. The corresponding regularization parameters when using the unit matrix as the regularization matrix is $4.51\ 10^{-21}$.

III. Results

The resolution as a function of the radius of the cylinder for 16, 8 and 4 excitation coils and different configurations for the receiving coils is depicted in figure 2 - 4. The absolute displacement of the centre of gravity for 16, 8 and 4 excitation coils and different configurations for the receiving coils are shown in figure 5 - 7. All simulations were performed with 40 dB signal-to-noise ratio.

IV. Discussion

The PSF was calculated for a cylindrical object using a voxel grid from x = -90 mm to 90 mm, from y = -90 mm to 90 mm and from z = -50 mm to 50 mm with an increment of 5 mm for Δx, Δy and Δz. The resolution in the centre is about 0.026 mm^{-1} and increases when moving to the border. As expected the use of 16 excitation coils and 32 receiving coils yields the best resolution which can be seen in figure 2. If 8 excitation coils and 16 receiving coils are used (see figure 3) better results are obtained with the configuration of the receiving coils on ring 2. In contrast, if 8 receiving coils are used better results are obtained when placing them on ring 1. When comparing figure 3 with figure 4 it can bee seen, that the results are contrariwise with respect to the receiving ring1 and ring 2.

The absolute displacement of the PSF is about 40 mm in the centre of the object and decreases to 5 mm when moving to the border. All calculations of the absolute displacement yield similar results except if 4 excitation coils and 8 receiving coils (see figure 7) are used. In these cases when moving from the centre to the border the absolute displacement first increases up to about 60 mm and then decreases to about 5 mm.

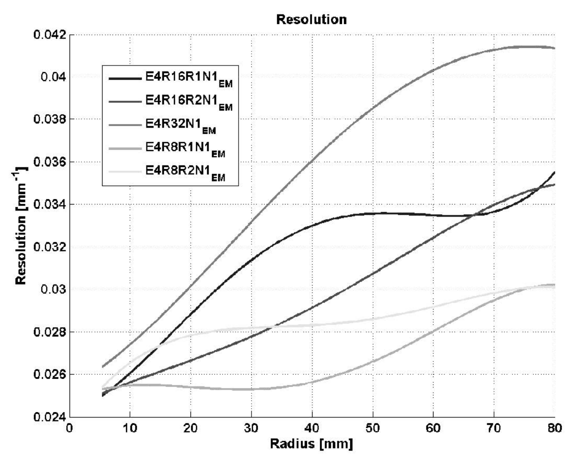

Fig. 4 Resolution in mm^{-1} as a function of the radius of the cylinder with 4 excitation coils, different configurations for the receiving coils and a SNR of 40 dB in the z-plane at z=0

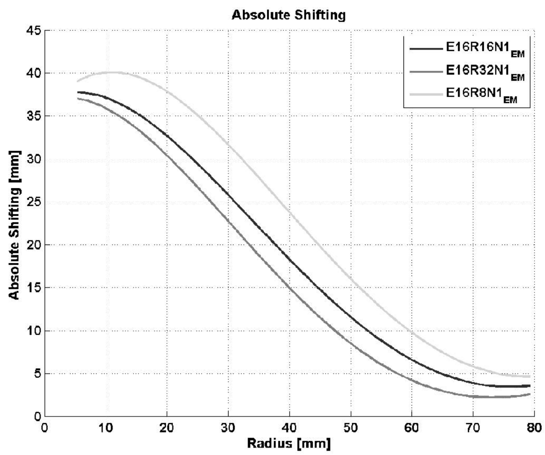

Fig. 5 Absolute displacement in mm as a function of the radius of the cylinder with 16 excitation coils, different configurations for the receiving coils and a SNR of 40 dB in the z-plane at z=0

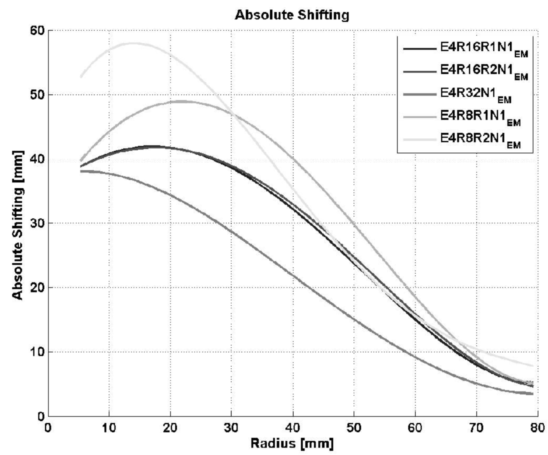

Fig. 7 Absolute displacement in mm as a function of the radius of the cylinder with 4 excitation coils, different configurations for the receiving coils and a SNR of 40 dB in the z-plane at z=0

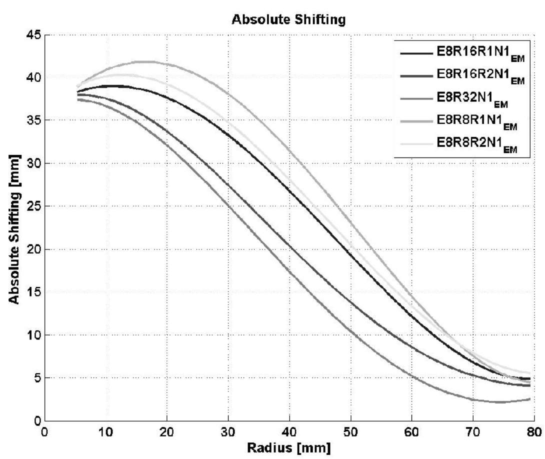

Fig. 6 Absolute displacement in mm as a function of the radius of the cylinder with 8 excitation coils, different configurations for the receiving coils and a SNR of 40 dB in the z-plane at z=0

The required SNR of 40 dB can be achieved with our MIT-system [7] when reducing the sampling bandwidth to about 0.2 Hz and driving the coils with 1 ampere.

V. Conclusion

Before designing a MIT device with a given number of excitation coils and receiving coils it is essential to know which coil configuration yields the best results with respect to the resolution and correctness of the reconstruction. Thus simulations in this way have to be carried out because the results show that the resolution and the displacement of a perturbation inside an object depends on the location within the object and on the chosen coil configuration.

References

1. Griffiths H 2001 Magnetic induction tomography. Meas. Sci. Technol. 12:1126–1131
2. Hansen P C (1998) Rank-deficient and ill-posed problems. Siam
3. Korjenevsky A, Cherepenin V and Sapetsky S (2000) Magnetic induction tomography: experimental realization. Physiol. Meas. 21: 89–94
4. Liu A, Dale A and Belliveau (2002) Monte Carlo Simulation Studies of EEG and MEG Localization Accuracy. Human Brain Mapping 16:47–62
5. Peyton A (1996) An overview of electromagnetic inductance tomography: Description of three different systems. Meas. Sci. Technol. 7:261–271
6. Scharfetter H, Hollaus K, Rosell-Ferrer J, Merwa R (2006) Single-Step 3-D Image Reconstruction in Magnetic Induction Tomography: Theoretical Limits of Spatial Resolution and Contrast to Noise Ratio. ANN BIOMED ENG DOI: 10.1007/s10439-006-9177-6
7. Scharfetter H, Kstinger A and Issa S (2007) Spectroscopic 16 channel magnetic induction tomograph: The new Graz MIT system. This issue
8. Tapp H and Peyton A (2003) A State of the Art Review of Electromagnetic Tomography. Proc. 3rd world congress on industrial process tomography 340–346

Address of the corresponding author:
Author: Robert Merwa
Institute: Institute of Medical Engineering
Street: Kronesgasse 5
City: Graz
Country: Austria
Email: merwa@tugraz.at